Original Research

Water Body Detection Analysis Using NDWI Indices Derived from Landsat-8 OLI

Emre Özelkan*

Department of Urban and Regional Planning, Faculty of Architecture and Design,
Çanakkale Onsekiz Mart University, Çanakkale, Turkey

Abstract

Normalized different water indices (NDWIs) derived from satellite images are commonly and successfully utilized in surface water body detection and mapping. In this study, the water body detection capability of three NDWI models ($NDWI_{(Green, NIR)}$, $NDWI_{(Green, SWIR1)}$ and $NDWI_{(Green, SWIR2)}$) generated using 28 multitemporal Landsat-8 OLI multispectral satellite images was analyzed for Atikhisar Dam Lake, the only water source of Çanakkalecity's central district in Turkey between 2013 and 2017. This study focused on two important open research questions: (i) Which NDWI model produces the most superior results? and (ii) How much does accuracy change in the use of 15 m and 30 m spatial resolution satellite data? For the accuracy analysis, area values extracted from the NDWI models were compared with in-situ lake area values as measured by the General Directorate of State Hydraulic Works (DSI). The results of this study show that as the lake area grows, discrimination of water from other classes is better with NIR region, and that the performance of $NDWI_{(Green, NIR)}$ is relatively better in terms of lake expansion effect. Results also indicate that hydrometeorological factors such as precipitation and evaporation and anthropogenic factors such as irrigation and daily consumption are decisive in lake area variations. The order of accuracy from high to low was found to be $NDWI_{(Green, NIR)}$, $NDWI_{(Green, SWIR1)}$ and $NDWI_{(Green, SWIR2)}$, and 15 m spatial resolution data generated better results than 30 m resolution.

Keywords: water body detection, remote sensing, NDWI, Landsat-8 OLI

Introduction

Water is the most important resource for sustaining life since it keeps the whole ecosystem alive and shapes human civilization [1, 2]. Water resource management will be the most important issue in the future as it is today, especially for arid and semi-arid regions [3]. Due to the increasing population and consequent increase in food requirements, global warming and climate change, precision water resources management is of much greater importance – especially in the organization of agricultural irrigation activities [4, 5]. However, effective water resource management is only possible with continuous monitoring [6, 7]. Satellite remote sensing is functional technology for monitoring natural resources such as water bodies and enables a time- and cost-effective monitoring of water resources with reliable data [8-10].

Several satellite remote sensing methods such as image classification, linear unmixing, single-band thresholding and water index are available to determine water bodies [11-14]. Since linear unmixing and image

*e-mail: emreozelkan@comu.edu.tr

classification depend on human expertise and comprise high computation and single-band thresholding based on limited information, water indices that can produce more accurate, faster and easier information than others are better at detecting water bodies [12]. The normalized difference water index (NDWI) introduced by McFeeters [15] is one of the most commonly used water indices to detect open surface water bodies and was firstcreated by the green and near-infrared (NIR) spectral bands of Landsat TM. Modified NDWI (MNDWI) comprising the green and short-wave infrared (SWIR) bands of Landsat TM was proposed by Xu [16] and is another commonly used index for water body detection. Another prominent water index was presented by Feyisa [17], whose automated water extraction index (AWEI) comprises five bands of Landsat TM (Blue, Green, NIR, SWIR1 and SWIR2) and is composed of two sub-indices ($AVEI_{sh}$ and $AVEI_{nsh}$). Many other studies proposing new methods and evaluation of water body detection indices are available in the literature [18-20]. The common feature in the design of the generated water indices is the absorption of water in the infrared region [11]. NDWI and MNDWI produced from Landsat images are at the top of the most-compared water indices in the literature [8, 12, 16]. While NDWI benefits from the high reflectance in NIR of vegetation and soil features [19], MNDWI can better separate built-up features from water [12]. While many researchers have found $NDWI_{(Green, SWIR)}$ to besuperior to $NDWI_{(Green, NIR)}$ [11, 12], others have found the opposite [2,8]. This is because quality may vary depending on the color, content and depth of the investigated water body [23].

In terms of spatial resolution, many studies have produced NDWI from either 15 m [12, 21] or 30 m [20, 23] resolution data. For accuracy assessment of methods, the general approach is to calculate the user's accuracy, producer's accuracy, overall accuracy and kappa coefficient of produced data using high spatial resolution images of the corresponding water body or GPS measurement for ground control point selection, as performed after image classification [17, 20].

In this study, the water body detection capability of the NDWI of McFeeters ($NDWI_{(Green, NIR)}$) and MNDWI of Xu ($NDWI_{(Green, SWIR)}$)were analyzed by using 28 multitemporal Landsat-8 Operational Land Imager (OLI) multispectral satellite images of Atikhisar Dam Lake in Çanakkale Province, Turkey between 2013 and 2017. Since Landsat-8 OLI has two SWIR bands, $NDWI_{(Green, SWIR1)}$ and $NDWI_{(Green, SWIR2)}$ were examined individually. At the same time, the examined NDWIs were produced from both 15 and 30 m resolution data. Unlike the general approach in accuracy assessment (i.e., using high spatial resolution images, GPS, etc.), the lake area values extracted by NDWI models were tested with *in-situ* measured lake area values. Lastly, the results were correlated with hydrometeorological factors such as precipitation and evaporation and anthropogenic factors such as irrigation and daily consumption. Based on the above assessments, in this study two important under-researched issues were addressed: (i) Which NDWI model produces the most superior results? and (ii) How much does the accuracy change in the use of 15 and 30 m spatial resolution satellite data? In the remainder of this paper the methods followed, including data, will first be presented. Thereafter, the paper will
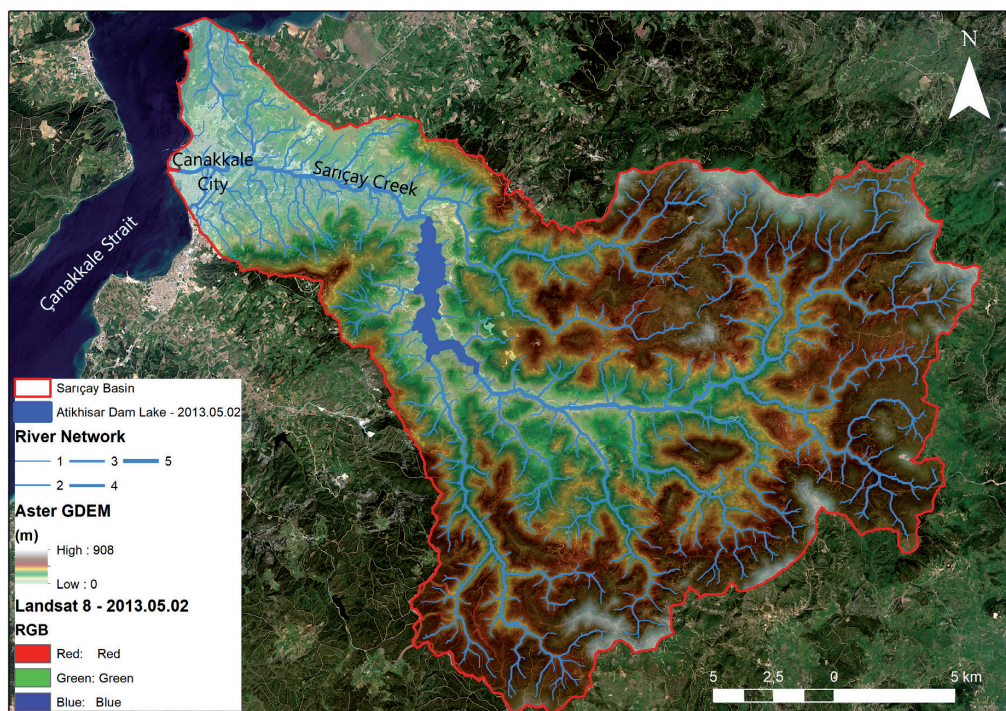

Fig. 1. Study area.

proceed with a detailed discussion of the results. Lastly, the paper will be completed with a summary of the major findings and recommendations.

Material and Methods

Study Area

The study area is Atikhisar Dam Lake within the borders of Çanakkale province in western Turkey located between 26°31'2.22"-26°33'10.30" eastern meridians and 40°7'36.31"-40°3'49.67" northern parallels (Fig. 1). Atikhisar Dam was built 1971-1975 as an earthfill body on Sarıçay Creek [24] at a height of 60 m above sea level and 11 km from Çanakkale city center, with a maximum area of 3.8 km^2 and volume of 53.5 hm^3 according to the General Directorate of State Hydraulic Works (DSI). Atikhisar Dam is a multi-purpose dam (supplying drinking water, irrigation, flood protection, etc.) and serves as the only water source of the central district of Çanakkale [6]. The study area is located in the subtropical Mediterranean climatic region [25] and under the influence of the Marmara climate, which is a transition zone between the Black Sea and Mediterranean [26]. Especially in winter, winds from the north cause temperatures to fall and winds blowing from the south bring rain to the region [27]. According to the Turkish State Meteorological Service long term data, the total annual precipitation and mean monthly temperature are 616 mm and 15°C. The rainiest month is December, with 106.8 mm precipitation, and the driest is August with 6.4 mm. The hottest month is July (25°C) and the coldest month is January (6.1°C). Hydrologically, according to Aster GDEM (global digital elevation map), the area of Sarıçay Basin where Atikhisar Dam Lake is located is 473.1 km^2. Sarıçay Basin does not have a dominant aspect direction due to its basin characteristics. High and sloping areas are situated south and east of the basin with maximum values of 908 m height and 45.7° slope. The area with the lowest height and slope is the plain where Sarıçay Creek flows freely into Çanakkale Strait (Dardanelles) and reaches its widest border between Atikhisar Dam Lake and the sea. The longest stream line comprises Sarıçay Creek within the basin, which is approximately 43 km, and 8.5 km of it lies within the dam.

Remote Sensing Data and Pre-Processing

Different dated 28 Level 1 U.S. Geological Survey (USGS) Landsat-8 Operational Land Imager (OLI) images were downloaded between 2013 and 2017 over the study area from the USGS's Earth Explorer data portal (Table 1). In selecting the remote sensing data, special attention was given to images with no cloud or fog over the study area. Since NDWI from reflectance images can generate more accurate results than NDWI from DN value images [8], surface reflectance images were utilized in this study. As an initial step, radiometric corrections, including the top-of-atmosphere (TOA) reflectance transformation of images were performed using ENVI software [21]. After that, the atmospheric correction of images was performed using Quick Atmospheric Correction (QUAC) of ENVI in order to obtain surface reflectance data [28]. Images were pan-sharpened in the 15m spatial resolution panchromatic band using the nearest-neighbor diffusion-based (NNDiffuse) pan sharpening algorithm [29]. Since this research was also concerned with the comparison of 15 m or 30 m spatial resolution data for water body detection, three NDWI models were employed for both spatial resolutions. 15 and 30 m resolutions of NDWI models will be referred as NDWI (15 m) (i.e. NDWI$_{(Green, NIR)}$ (15 m), NDWI$_{(Green, SWIR1)}$ (15 m) and NDWI$_{(Green, SWIR2)}$ (15 m)) and NDWI (30 m) (i.e., NDWI$_{(Green, NIR)}$ (30 m), NDWI$_{(Green, SWIR1)}$ (30 m) and NDWI$_{(Green, SWIR2)}$ (30 m)) respectively inthe remainder of the paper. As a result,
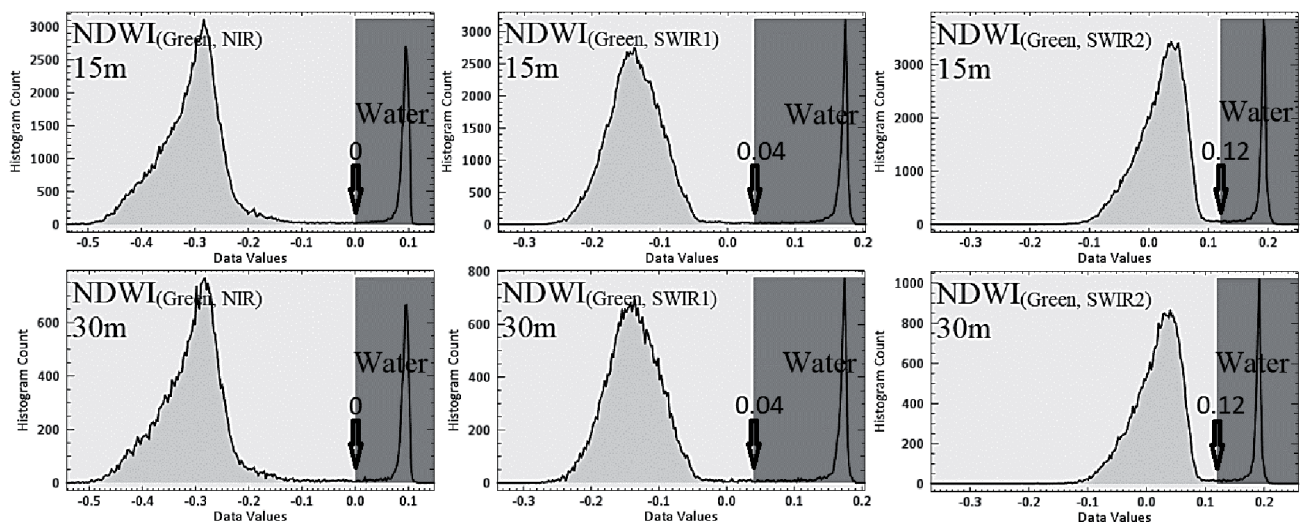

Fig. 2. Thresholding of 2013.05.02 NDWI models.

2 (15 and 30 m resolution data) × 3 (NDWI models) × 28 images = 168 water index data were produced. The examined NDWI models based on McFeeters [15] and Xu [16] are as follows:

$$NDWI_{(Green, NIR)} = (Green - NIR)/(Green + NIR) \quad (1)$$

$$NDWI_{(Green, SWIR1)} = (Green - SWIR1)/(Green + SWIR1) \quad (2)$$

$$NDWI_{(Green, SWIR2)} = (Green - SWIR2)/(Green + SWIR2) \quad (3)$$

Green is the 3rd band, NIR is the 5th band, SWIR1 is the 6th band and SWIR2 is the 7th band of Landsat-8 OLI. For distinguishing water and non-water areas, NDWI threshold values can be successfully designated both manually and automatically [8, 11, 16, 18, 30]. In this study, manual designation was preferred in consideration of the water and non-water classes. For $NDWI_{(Green, NIR)}$, $NDWI_{(Green, SWIR1)}$ and $NDWI_{(Green, SWIR2)}$, threshold values for resolution were found as 0, 0.04 and 0.12, respectively (Fig. 2). The threshold values are indicated by an arrow in the histograms (Fig. 2). On the histograms, the dark greypart on the right side of the threshold is water, and on the left is the distribution of non-water pixels. If there were still mixed pixels over the classes out of water, they were manually cleaned.

Validation Data

The NDWI model area results were evaluated by comparison with *in-situ* water area measurement values of the Turkish General Directorate of State Hydraulic Works. All measurements were performed on the first day of the month. The acquisition dates of the satellite images cannot always be the same as the lake measurement days. Deviations of data acquisition dates from lake measurement days are shown in Table 1. Note that deviations of up to 7 days were included in the study. Additionally, meteorological data from the Turkish State Meteorological Service were used to interpret the model results.

Data Analysis

The performance of the NDWI models was tested utilizing root mean square error (RMSE) and Pearson's correlation coefficients (R) to correlate the computed data (lake area values derived from NDWI models) with validation data (lake area values derived from *in-situ* measurements). As previously mentioned, each of 6 different data sets' (3 NDWI models with 2 different resolutions each) of water body area values were compared with validation data separately. Each data set contained 28 differently dated values and was compared with the corresponding *in-situ* measurement values.

Table 1. List of Landsat-8 OLI images used.

No	Path/Row	Image Acquisition Date	Day Difference from *In-Situ* Measurement Date
1	181/32	2013.05.02	1
2	182/32	2013.06.26	5
3	182/32	2013.08.29	3
4	182/32	2013.09.30	1
5	182/32	2013.10.25	7
6	181/32	2014.04.03	2
7	182/32	2014.05.28	4
8	182/32	2014.06.29	2
9	181/32	2014.08.25	7
10	182/32	2014.11.04	3
11	182/32	2015.07.02	1
12	181/32	2015.07.27	5
13	181/32	2015.08.28	4
14	182/32	2015.12.25	7
15	181/32	2016.03.07	6
16	182/32	2016.03.30	2
17	182/32	2016.06.02	1
18	181/32	2016.06.27	4
19	181/32	2016.08.30	2
20	181/32	2016.10.01	0
21	181/32	2016.11.02	1
22	182/32	2017.01.28	4
23	182/32	2017.04.02	1
24	182/32	2017.05.04	3
25	181/32	2017.06.30	1
26	181/32	2017.09.02	1
27	181/32	2017.10.04	3
28	182/32	2017.10.27	5

Results and Discussion

The water body detection capability of $NDWI_{(Green, NIR)}$, $NDWI_{(Green, SWIR1)}$ and $NDWI_{(Green, SWIR2)}$ derived from Landsat-8 OLI was examined in this study. NDWIs were produced from both 15 and 30 m resolution data. Each of the 6 data sets (3 NDWI models with 2 different spatial resolutions each) were compared with *in-situ* measured lake area values. Consequently, findings were evaluated by considering the water input-output parameters.

In-situ Measurements

When the used *in-situ* measured values are examined, we found that the lake generally reaches its greatest limits at the end of the rainy period and its narrowest limits at the end of the dry period. However, dates for the minimum and maximum areas may vary, and the most decisive elements are hydrometeorological factors such as precipitation and evaporation, and anthropogenic factors such as irrigation and daily consumption. In evaluating the values of the data set, the smallest area was formed on October 27, 2017 with 2.135 km². Although October is normally within the rainy season, the main reason for the water body of the lake being narrow on 2017.10.27 was that the precipitation in September, the first month of the rainy period, declined by about 70% (i.e., a meteorological drought) compared to the long-term data. The second reason was water used for agricultural irrigation in September. Conversely, the largest limit was formed on May 2, 2013, when it was not yet the end of the rainy season, with 3.692 km². The most important factor in this early formation was the excessive precipitation in January, February and April, which is about twice the long-term average.
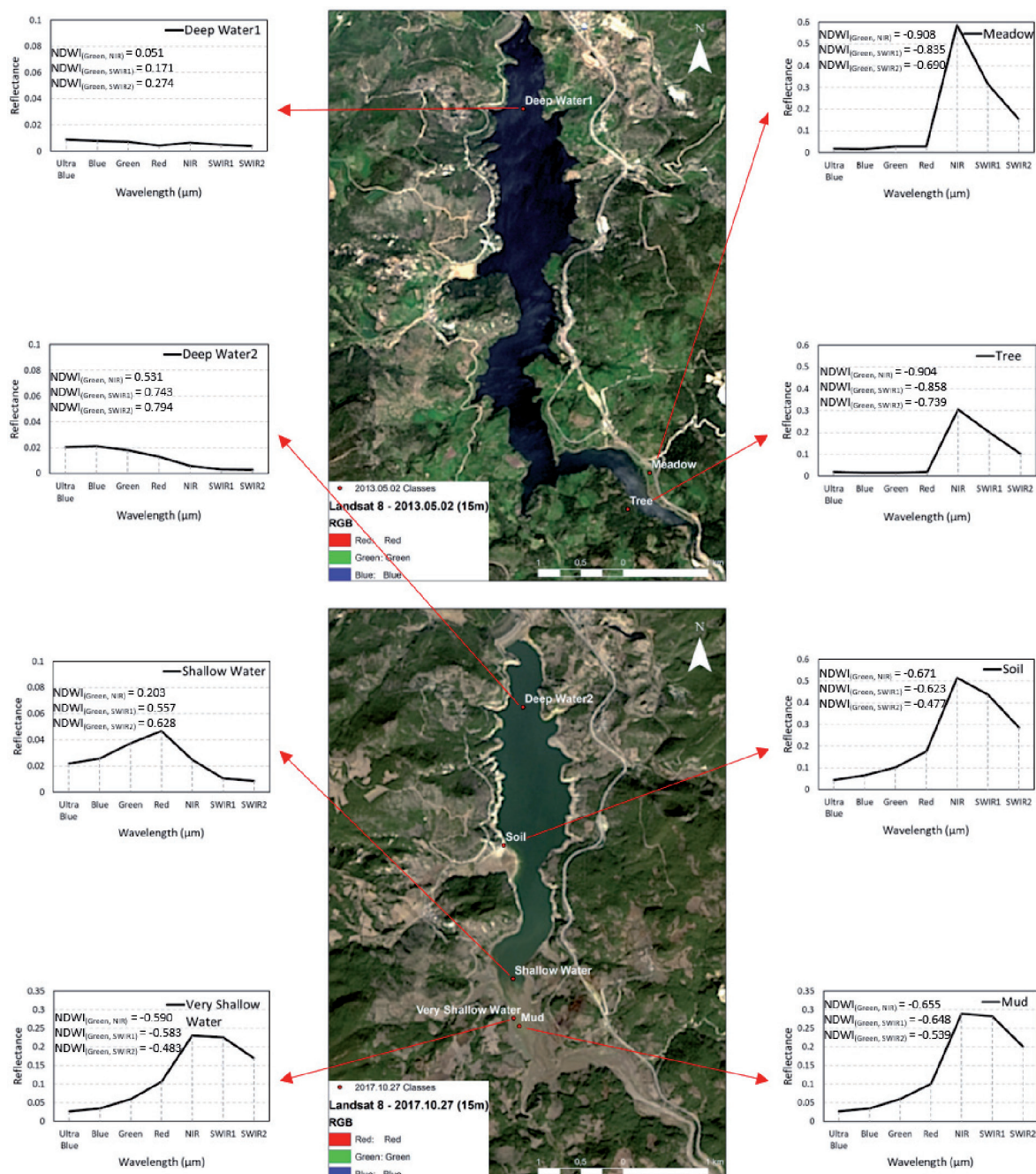

Fig. 3. Spectral signatures of different land cover classes for 2013.05.02 and 2017.10.27.

Lake Area and Environment

While the adjacent classes to the lake area are trees, soil and meadows, the lake area consists of water and mud varying seasonally due to meteorological conditions and water consumption. NDWI models, which are formed from sample spectral curves (i.e.,spectral signatures) in and adjacent to the lake area, successfully produced water classes as positive and other classes as negative (Fig. 3). All classes were verified by using Google Earth's high spatial resolution images. Deep Water1, Deep Water2, Shallow Water, and Very Shallow Water were the classes examined. Deep Water classes were from almost the deepest point of the lake. Deep Water1 from 2013.05.02 had the maximum lake area and the color of the water body was blue. Deep Water2 from 2017.10.27 had the minimum lake area and the color of the water was greenish-blue. Blue water has lower reflectance and greenish-blue water has higher reflectance in visible bands. Shallow water has higher reflectance in the green and red bands due to the bottom effect and can still be classified as water. The spectral signature of very shallow water behaves like that of mud, having a low reflectance in visible bands and high in infrared bands, and cannot be assigned as belonging in the water class by all NDWI models (Fig. 3).

Performance of NDWI Models

The area results of all NDWI models have a high positive correlation with *in-situ* measured area values (Fig. 4). Moreover, all NDWI models produced maximum and minimum values on the same dates as *in-situ* measurements. Even though the $NDWI_{(Green, SWIR1)}$ (30 m) and $NDWI_{(Green, SWIR2)}$ (15 m) generated the lowest and highest correlated resul ts, respectively, R values may not be determinative for detecting the most superior NDWI model since the difference between minimum ($R = 0.987$) and maximum ($R = 0.991$) correlations is just 0.004. According to significance probabilities (p) of ANOVA (analysis of variance) (i.e., significance F (SF)), all correlations have almost 100% confidence level.

It can be seen that the differences between the performance of the NDWI models can be distinguished by the RMSE results (Fig. 4, Table 2). The lowest RMSE values were obtained by $NDWI_{(Green, NIR)}$, then $NDWI_{(Green, SWIR1)}$, and the highest RMSE values were obtained by $NDWI_{(Green, SWIR2)}$. In each NDWI model, 15 m resolution generated more accurate data than the 30 m. The 15 m resolution of $NDWI_{(Green, NIR)}$, $NDWI_{(Green, SWIR1)}$, and $NDWI_{(Green, SWIR2)}$ were 13.433%, 9.774% and 3.646% better than the 30 m models, respectively. 15 m was expected to be far superior to what 30 m had done especially for NDWI with SWIR bands. These ratios
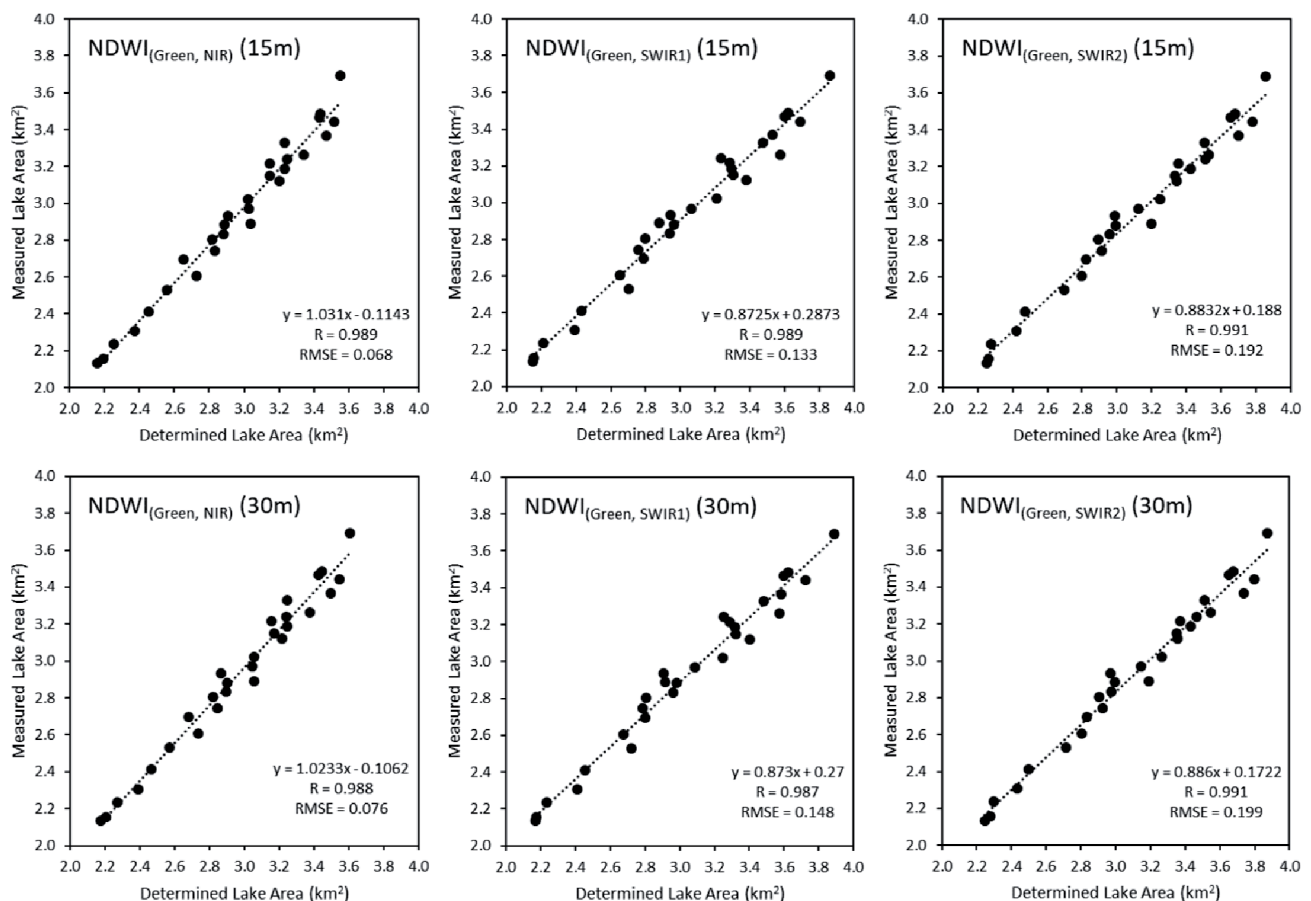

Fig. 4. Correlations between *in-situ* measurements and NDWI model values.

Table 2. Mean, standard deviation (Stdv) and RMSE values of complete data setof NDWI and in-situ measurement areas.

Resolution (m)	NDWI(Green, NIR)		NDWI(Green, SWIR1)		NDWI(Green, SWIR2)		*In-situ* Measurement
	15	30	15	30	15	30	
RMSE (km²)	0.068	0.076	0.133	0.148	0.192	0.199	-
Mean (km²)	2.955	2.969	3.032	3.050	3.107	3.115	2.932
Stdv (km²)	0.412	0.415	0.483	0.481	0.487	0.486	0.430

may show that utilizing the pan-sharpening algorithm NNDiffuse is better for NIR.

On the other hand, RMSE values have a positive correlation witht he mean and standard deviation values. When the mean and standard deviations increase, RMSE also increases. RMSE decreases as the measurement values approach the mean and standard deviation values (Table 2). It was determined that the mean and standard deviation values closest to the *in-situ* measurements were reached with McFeeter's NDWI and the farthest values were reached with Xu's NDWI with SWIR2. The 15 m spatial resolution of $NDWI_{(Green, NIR)}$ produced the closest result with 0.0784% and 4.186% deviations from the mean and standard deviation values, while the 30 m spatial resolution of $NDWI_{(Green, SWIR2)}$ generated the farthest result with 6.241% and 13.023% deviations.

As the results of Table 2 indicate, RMSE increases with increasing water body area. The correlations between the NDWI models' values and the absolute difference of the NDWI models' output values from measured values were examined. The results that are shown in Fig. 5 seem to confirm the correlation between RMSE and lake area, especially for $NDWI_{(Green, SWIR1)}$ and $NDWI_{(Green, SWIR2)}$, with a significant correlation of around 0.7 R. However, the $NDWI_{(Green, NIR)}$ model results were less influenced than other NDWI models by area enlargement, as seen in Fig. 5. On the other hand, for 2013.05.02, the gradual and consecutive enlargement of the lake area as a result of the model performances from $NDWI_{(Green, NIR)}$ to $NDWI_{(Green, SWIR2)}$ can be seen in Fig. 6. While $NDWI_{(Green, NIR)}$ (15m) was found to be the best model with 3.606 km², the calculated areas increase and diverge consecutively from the *in-situ*
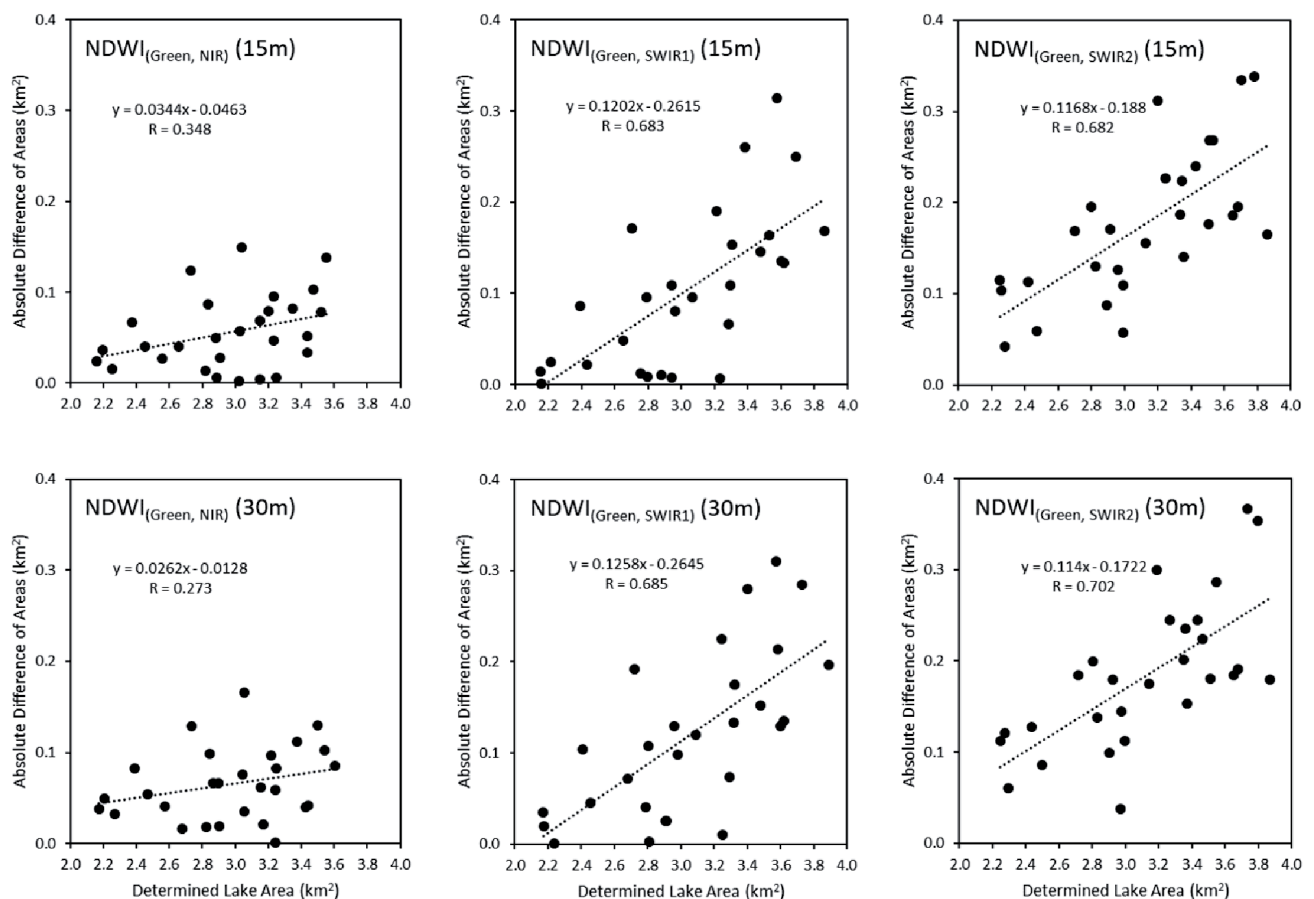

Fig. 5. Correlations between absolute difference and NDWI model values.

measured values of 3.692 km^2 (Fig. 6), where the faultiest is NDWI$_{(Green, SWIR2)}$ but close to NDWI$_{(Green, SWIR1)}$. For the smaller areas, the success of the models may not be sequential (i.e., best: NDWI$_{(Green, NIR)}$, mid: NDWI$_{(Green, SWIR1)}$, and worst: NDWI$_{(Green, SWIR2)}$) as they do in large lakes (Fig. 6). In Fig 6, since the areas of NDWI$_{(Green, SWIR1)}$ and NDWI$_{(Green, SWIR2)}$ are so close, color discrimination can be recognized in the outermost areas and in small amounts.

The results indicate that when the lake expands, water is in contact with other land cover classes such as trees, meadows and soil on its border. High reflection of vegetation and soil in NIR allows NDWI$_{(Green, NIR)}$ to be less affected by this interaction on its border and to give more accurate results. The lack of built-up classes adjacent to the water mass increases the accuracy of NDWI$_{(Green, NIR)}$, which normally cannot sufficiently suppress the reflectance from built-up areas. NDWI$_{(Green, SWIR1)}$ and NDWI$_{(Green, SWIR2)}$ perform better for smaller lake areas owing to less interaction with classes adjacent to the water body (Fig. 6).

In addition, it may be thought that classification errors arising from this interaction are caused by spatial resolution. However, where the area is large and the interaction between classes is high, the accuracy difference between the 15 m and the 30 m spatial resolution is similar to that in small areas.

If there is a structure that creates shadows in the area and the images are cloudy, this could cause an error in determining the water body [2]. Although a shadow effect originating from trees could not be determined in this study area; after expansion of the lake, whether the
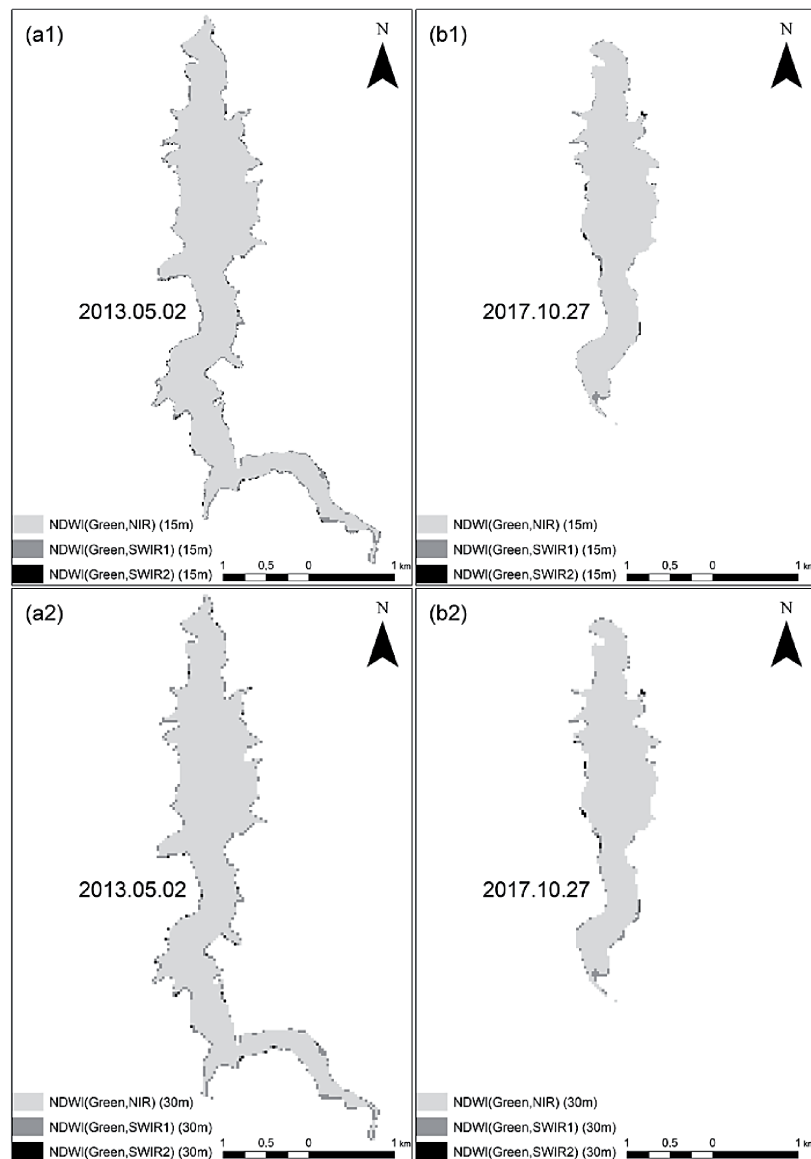

Fig. 6. Results from 2013.05.02 and 2017.10.27 Landsat-8 OLI image (Fig. 3): a1) 2013.05.02 dated 15 m spatial resolution NDWI model results, a2) 2013.05.02 dated 30 m spatial resolution NDWI model results, b1) 2017.10.27 dated 15 m spatial resolution NDWI model results, and b2) 2017.10.27 dated 30 m spatial resolution NDWI model results (light grey to black in order of NDWI$_{(Green, NIR)}$, NDWI$_{(Green, SWIR1)}$ and NDWI$_{(Green, SWIR2)}$, respectively).

water enters the forest areas or not may be determined by field studies.

Effect of Data Acquisition Date and Water Input-Output

When Table 2 is examined again, it is seen that RMSE values of the 6 NDWI models correspond to 2.285%, 2.592%, 4.536%, 4.980%, 6.548% and 6.787% of the mean of the lake area (2.932 km^2). Although errors are not very high, when the size of the study area, uncomplicated topographical and formal structure and several land cover classes in and adjacent to the lake are considered, the accuracy could be higher. So far, the causes of these errors have been sought from the NDWI model (i.e., remote sensing) framework. As a next step, the time difference between the imaging and measurement dates and the water input-output occurring at this time are also evaluated. Water input-output data were gathered from the General Directorate of State Hydraulic Works and the Turkish State Meteorological Service. Table 1 includes the day difference between *in-situ* measurement date and acquisition date of the image. As already mentioned, all lake measurements were made on the first day of the month. Only one of the image acquisitions is the same date as the *in-situ* measurement. The images with different dates were utilized up to 7 days, and the mean day difference from the measurement date is 3 days. Sometimes the error may be high even though the time difference is low, while in some cases it is vice versa.

Some of the remarkable results from the superior model NDWI$_{(Green, NIR)}$ (15 m), whose absolute differences of the NDWI model's output values from the measured values were greater than 0.068 km^2 RMSE, were examined as follows. Firstly, however, it is worth remembering that this dynamic and rapidly changing dam lake is the only water source of the city and its usage is multipurpose.

– On 2013.05.02, although there was no precipitation for 1 day, the area determined by NDWI was 0.086 km^2 lower than the *in-situ* measured lake area. Since the dam area was around its maximum, water was probably released. According to the dam's operation report, the water outlet from the bottom was 1.81 hm^3 in May 2013.
– On 2013.10.25, 7 days before measurement day, the NDWI result was 0.098 km^2 larger than the measured amount. This error is less than expected since this 7-day period had no precipitation and the evaporation was low due to autumn temperatures.
– On 2014.11.04, NDWI produced a water area that was 0.129 km^2 larger than the value measured 3 days before. The precipitation was just 0.6 mm during this 3-day period and insufficient for feeding the lake. On the other hand, 111 mm of precipitation occurred in September and October 2014, which probably contributed to increasing underground water, a vital source for the lake area.

– On 2015.07.27, 5 days before the measured day, the area determined by NDWI was 0.112 km^2 larger than the *in-situ* measured lake area. Although there was no precipitation for 5 days, a total of 0.81 hm^3 open water surface evaporation and 3.43 hm^3 irrigation usage occurred in July 2015.
– On 2015.12.25, 7 days prior to the measured day, the NDWI result was 0.166 km^2 higher than the measured figure. This was the maximum error determined in this study. During this 7-day period there was no precipitation, but constant consumption of the available water by the city took place.
– On 2016.03.07, due to 19.8 mm of precipitation within 6 days, the expansion of the lake area since the beginning of the month caused an NDWI mapping error of 0.130 km^2.
– On 2016.06.02, just 1 day ahead of the measured day, the NDWI result was 0.083 km^2 smaller than the measured value. Initially, this error was more than expected, but when the ongoing agricultural irrigation and evaporation due to summer conditions are taken into account, the result makes sense.
– On 2016.06.27, although there was 33.5 mm precipitation between 2016.06.27 (the imaging day) and the beginning of the month, the difference was 0.096 km^2 under the expected error. This may be due to the 0.7 hm^3 of monthly evaporation in June 2016.

The examples cited above, as well as the quality of the remote sensing data and the preferred NDWI model, not only emphasize the importance of the timing between satellite imaging and *in-situ* measurement, but also the enormous influence of water input-output that occurred in the possible time difference between satellite imaging and *in-situ* measurement of the lake.

Conclusions

Water indices derived from satellite data are effectively used in water resource management. This case study analyzed the water body detection capabilities of three NDWI models: NDWI$_{(Green, NIR)}$, NDWI$_{(Green, SWIR1)}$ and NDWI$_{(Green, SWIR2)}$ of Landsat-8 OLI imagery at the Atikhisar Dam Lake in Çanakkale Province, Turkey. The effect of spatial resolution on NDWI performance was tested by using both the 15 and the 30 m resolution data. Unlike generally used methods, the accuracy assessment of the detected water areas by NDWI was not performed with common classification accuracy assessment methods; rather, the detected area values were tested with *in-situ* measured values. Consequently, the results were assessed by considering water input-output parameters. The main findings of this study are as follows.

– NDWI$_{(Green, NIR)}$ was the best NDWI model for detecting the water body.
– The fact that the structure of the lake and its border is completely natural (i.e., water, trees, meadows,

mud and soil) was a major factor in the success of $NDWI_{(Green, NIR)}$.

- When the lake area increases and water interacts with the lake boundary land cover classes, the performances of $NDWI_{(Green, SWIR1)}$ and $NDWI_{(Green, SWIR2)}$ were more affected than $NDWI_{(Green, NIR)}$.
- All data sets of the NDWI models with a spatial resolution of 15 m produced better results than 30 m.
- The time differences between remote sensing data acquisition and measurement dates can increase the water body area detection error in dynamic lakes such as the one studied.
- The water input-output, i.e., hydrometeorological factors such as precipitation and evaporation and anthropogenic factors such as irrigation and daily consumption, was found to be decisive in these errors.

In this study, a comprehensive analysis of NDWI models was performed within an existing limited data set. Future studies may be more comprehensive by utilizing more lake data from other parts of Turkey and assessing new water indices. As a next step, the effect of pan-sharpening and atmospheric correction on spatial and spectral information and different algorithms may be tested for image processing. Additionally, statistical accuracy (i.e., comparing the NDWI's area with *in-situ* measurement area) and thematic accuracy (i.e., comparing the NDWI classification image with a high-resolution image) of the water area may be evaluated.

Acknowledgements

Conflict of Interest

The authors declare no conflict of interest.

References

1. FENG M., SEXTON J.O., CHANNAN S., TOWNSHEND J.R. A global, high-resolution (30-m) inland water body dataset for 2000: first results of a topographic–spectral classification algorithm. International Journal of Digital Earth, **9** (2), 113, **2016**.
2. ACHARYA T.D., LEE D.H., YANG I.T., LEE J.K. Identification of water bodies in a Landsat 8 OLI image using a J48 decision tree. Sensors, **16** (7), 1075, **2016**.
3. DEMIREL K., KAVDIR Y. Effect of soil water retention barriers on turfgrass growth and soil water content. Irrigation Science, **31** (4), 689, **2013**.
4. GENC L., DEMİREL K., ÇAMOGLU G., ASIK S., SMITH S. Determination of plant water stress using spectral reflectance measurements in watermelon (citrullus vulgaris). American-Eurasian Journal of Agricultural & Environmental Sciences, **11** (2), 296, **2011.**
5. ÇAMOĞLU G., DEMİREL K., GENC L. Use of infrared thermography and hyperspectral data to detect effects of water stress on pepper. Quantitative InfraRed Thermography Journal, **15** (1), 81, **2018**.
6. ÖZELKAN E., KARAMAN M. The analysis of the effect of meteorological and hydrological drought on dam lake via multitemporal satellite images: a case study in Atikhisar Dam Lake (Çanakkale). Omer Halisdemir University Journal of Engineering Sciences, **7** (2), 1023, **2018**.
7. KARAMAN M., BUDAKOGLU M., UCA AVCI Z.D., ÖZELKAN E., BULBUL A., CIVAS M., TASDELEN S. Determination of seasonal changes in wetlands using CHRIS/Proba Hyperspectral satellite images: A case study from Acigöl (Denizli), Turkey. Journal of Environmental Biology, **36**, 73, **2015**.
8. LIU Z., YAO Z., WANG R. Assessing methods of identifying open water bodies using Landsat 8 OLI Imagery. Environ Earth Sci, **75**, 873, **2016**.
9. KARAMAN M., ÖZELKAN E., TASDELEN S. Influence of basin hydrogeology in the detectability of narrow rivers by Sentinel2-A satellite images: A case study in Karamenderes (Çanakkale). Journal of Natural Hazards and Environment, **4**, 140, **2018**.
10. KALE S., ACARLI D. Shoreline change monitoring in Atikhisar reservoir by using remote sensing and geographic information system (GIS). Fresenius Environmental Bulletin, **28** (5), 4329, **2019**.
11. JI L., ZHANG L., WYLIE B. Analysis of dynamic thresholds for the normalized difference water index. Photogrammetric Engineering & Remote Sensing, **75** (11), 1307, **2009**.
12. DU Z., LI W., ZHOU D., TIAN L., LING F., WANG H., GUI Y., SUN B. Analysis of Landsat-8 OLI imagery for land surface water mapping. Remote Sensing Letters, **5** (7), 672, **2014**.
13. GÜRSOY Ö., ATUN R. Investigating surface water pollution by integrated remotely sensed and field spectral measurement data: A case study. Polish Journal of Environmental Studies, **28** (4), 2139, **2019**.
14. GÜRSOY Ö., BIRDAL A., ÖZYONAR F., KASAKA E. Determining and monitoring the water quality of Kizilirmak River of Turkey: First results. ISPRS - International Archives of the Photogrammetry, Remote Sensing and Spatial Information Sciences, **XL-7/W3**, 1469, **2015**.
15. MCFEETERS S.K. The use of normalized difference water index (NDWI) in the delineation of open water features. International Journal of Remote Sensing, **17**, 1425, **1996**.
16. XU H. Modification of normalised difference water index (NDWI) to enhance open water features in remotely sensed imagery. International Journal of Remote Sensing, **27** (14), 3025, **2006**.
17. FEYISA G.L., MEILBY H., FENSHOLT R., PROUD S.R. Automated water extraction index: A new technique for surface water mapping using Landsat imagery. Remote Sensing of Environment, **140**, 23, **2014**.
18. JI L., GENG X., SUN K., ZHAO Y., GONG P. Target detection method for water mapping using Landsat 8 OLI/TIRS imagery. Water, **7** (2), 794, **2015**.

19. KO B.C., KIM H.H., NAM J.Y. Classification of potential water bodies using Landsat 8 OLI and a combination of two boosted random forest classifiers. Sensors, **15** (6), 13763, **2015**.

20. MISHRA K., PRASAD P.R.C. Automatic extraction of water bodies from Landsat Imagery using perceptron model. Journal of Computational Environmental Sciences, **2015 (903465)**, 1, **2015**.

21. YANG Y., LIU Y., ZHOU M., ZHANG S., ZHAN W., SUN C., DUAN Y. Landsat 8 OLI image based terrestrial water extraction from heterogeneous backgrounds using a reflectance homogenization approach. Remote Sensing of Environment, **171**, 14, **2015**.

22. SHENG Y., SONG C., WANG J., LYONS E.A., KNOX B.R., COX J.S., GAO F. Representative lake water extent mapping at continental scales using multi-temporal Landsat-8 imagery. Remote Sensing of Environment, **185**, 129-, **2016**.

23. FISHER A., FLOOD N., DANAHER T. Comparing Landsat water index methods for automated water classification in eastern Australia. Remote Sensing of Environment, **175**, 167, **2016**.

24. AKBULUT M., ODABASI D.A., KAYA H., CELIK E.S., YILDIRIM M.Z., ODABASI S., SELVI K. Changing of mollusca fauna in comparison with water quality: Saricay Creek and Atikhisarreservoir models (Canakkale-Turkey)", Journal of Animal and Veterinary Advances, **8** (12), 2699, **2009**.

25. ALTAN G, TÜRKEŞ M. Hydroclimatologic Characteristics of the forest fires occurred at the Çanakkale district and relationship with climate variations. Aegean Geographical Journal, **20** (2), 1, **2015**.

26. SENSOY S., DEMIRCAN M., ULUPINAR Y., BALTA Z. 2008. Climate of Turkey. Turkish State Meteorological Service Report. Available online: https://www.mgm.gov.tr/FILES/genel/makale/13_turkiye_iklimi.pdf (accessed on 12.10.2018) [In Turkish].

27. ILGAR R. Drought status and trends in the Dardanelles and the standardized precipitation index determination. Marmara Geographical Review, **0** (22), 183, **2010**.

28. BERNSTEIN L.S., ADLER-GOLDENS.M., SUNDBERG R.L., LEVINE R.Y., PERKINS T.C., BERK A., RATKOWSKI A.J., FELDE G., HOKE M.L. Validation of the QUick atmospheric correction (QUAC) algorithm for VNIR-SWIR multi- and hyperspectral imagery. Proc. SPIE, **5806**, 668, **2005**.

29. SUN W., CHEN B., MESSINGER D. Nearest-neighbor diffusion-based pan-sharpening algorithm for spectral images. Opt. Eng. **53** (1), 013107(1-11), **2014**.

30. OZTURK D., SESLI F.A. Determination of temporal changes in the sinuosity and braiding characteristics of the Kizilirmak River, Turkey. Pol. J. Environ. Studies, **24** (5), 2095, **2015**.